

ANALYSIS OF THE SCATTERING MECHANISM IN AN  
ABRUPTLY ENDED ROD DIELECTRIC WAVEGUIDE. APPLICATION TO THE DETERMINATION  
OF THE CHARACTERISTICS OF DIELECTRIC RESONATORS

PH. GELIN, M. PETENZI, P. KENNIS, J. CITERNE

"Centre hyperfréquence & Semiconducteur" L.A. au CNRS 287 Université de LILLE I  
Bâtiment P4 - BP 36 59650 VILLENEUVE D' ASCQ FRANCE

ABSTRACT

The scattering mechanism of the magnetic dipolar mode  $TE_{01}$  incident in an abruptly ended rod dielectric waveguide is analysed by means of a novel integral formulation. The accurate numerical solution is obtained from an iterative procedure based on successive scattering approximation. In the second part of this paper, we applied the previous results to determine the characteristics of circular dielectric resonators.

INTRODUCTION

In the last few years, the availability of dielectric materials with high relative permittivity has given a great impulse to the use of dielectric resonators in microwave integrated circuits (pass-band filters, stabilized solid state sources...). So many authors have published approximate theories able to calculate the resonant frequency of cylindrical dielectric resonators [1][2]. These theories assume that the energy is stocked inside and close to the resonator so that its radiation properties cannot be taken into consideration. Professor VAN BLADEL's analysis alone can determine the radiation quality factor of dielectric resonators [3].

In this paper, we present a quite different and new analysis which proceeds in two steps. First, we study separately the electromagnetic behavior of an abruptly ended circular dielectric waveguide together with the behavior of a substrate plug ended one. Secondly, we take into account the interaction between such discontinuities to formulate the dielectric resonator problem.

DISCONTINUITIES ANALYSIS

Our purpose is to derive the resonant frequency together with the radiation  $Q$  factor of the magnetic dipole mode of a cylindrical dielectric resonator. To do so, we focus our attention on the reflection and scattering coefficients of the  $TE_{01}$  circular waveguide mode incident on the plugged rod of the fig. 1. The plugged geometry can be changed into the abruptly ended rod configuration by choosing  $L = \infty$  together with  $\epsilon_{r1} = 1$ .

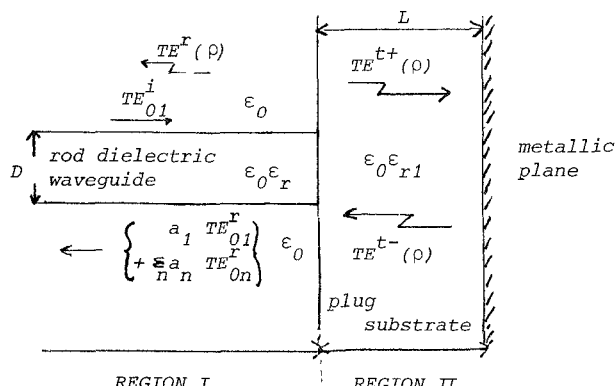


figure 1

In the discontinuity plane  $z=0$ , we have to match the tangential electric and magnetic fields which are azimuthal (subscript  $\theta$ ) and radial (subscript  $r$ ) respectively. The continuity relations can be expressed as:

$$\begin{bmatrix} E_{\theta 1}^i \\ H_{r1}^i \end{bmatrix} + a_1 \begin{bmatrix} E_{\theta 1}^r \\ H_{r1}^r \end{bmatrix} + \sum_n a_n \begin{bmatrix} E_{\theta n}^r \\ H_{rn}^r \end{bmatrix} + \int_0^\infty q^r(\rho) \begin{bmatrix} E_{\theta}^r(\rho) \\ H_r^r(\rho) \end{bmatrix} d\rho \\ = \int_0^\infty q^{t+}(\rho) \begin{bmatrix} E_{\theta}^{t+}(\rho) \\ H_r^{t+}(\rho) \end{bmatrix} d\rho + \int_0^\infty q^{t-}(\rho) \begin{bmatrix} E_{\theta}^{t-}(\rho) \\ H_r^{t-}(\rho) \end{bmatrix} d\rho$$

The fields of the left-hand side of the above equation is a superposition of the incident guided  $TE_{01}$  mode (superscript  $i$ ), of the reflected  $TE_{01}$  guided modes and of the reflected continuous  $TE$  modes (superscript  $r$ ) in region I. On the right-hand side of this equation, are superposed the transmitted continuous  $TE$  modes in region II (superscript  $t+$  for the modes incident toward the metallic plane, superscript  $t-$  for the other ones reflected on the metallic plane). The constant  $a_1$  is the reflection coefficient of the incident  $TE_{01}$  mode while alternately, the constants  $a_n$  ( $n > 1$ ) are the coupling coefficients of the incident mode on reflected and guided modes  $TE_{0n}$  in region I.

The functions  $q^r(\rho)$  are the coupling amplitudes of the backward scattered continuous modes in region I. Backward and forward coupling amplitudes of transmitted continuous modes in region II, are denoted by the functions  $q^{t+}(\rho)$  and  $q^{t-}(\rho)$ , respectively. The variable

of these functions is either the transverse wave-number outside the rod in region I, or the transverse wavenumber inside the dielectric plug. If we denote  $\beta(\rho)$  and  $\beta_1(\rho)$  the phase constants of the continuous modes in region I and in region II respectively, then, these transverse wavenumbers can be defined either as:

$$\rho^2 = k_0^2 - \beta^2(\rho) \quad \text{or as} \quad \rho^2 = k_0^2 \epsilon_{r1} - \beta_1^2(\rho) \\ \text{with} \quad k_0^2 = \omega^2 \mu_0 \epsilon_0$$

The boundary condition at the metallic plane ( $z=L$ ) provides a simple relation between the functions  $q^{t+}(\rho)$  and  $q^{t-}(\rho)$  namely:

$$q^{t-}(\rho) = -q^{t+}(\rho) \cdot e^{-2j\beta_1(\rho)L}$$

By introducing an indicator  $\Delta$  such as  $\Delta = 1$  if the metallic plane exists, and such as  $\Delta = 0$  if the metallic plane is removed, we can treat the abruptly ended circular dielectric waveguide together with the substrate plugged one by rewriting the above boundary condition as:  $q^{t-}(\rho) = -q^{t+}(\rho) \cdot \Delta \cdot e^{-2j\beta_1(\rho)L}$

Taking account of the simple relations in the two regions between the backward and forward electric and magnetic fields [4], the general mode matching equations at  $z = 0$  can consequently take the form:

$$\begin{aligned} & \left[ \begin{matrix} 1+a_1 \\ \beta_1(1-a_1) \end{matrix} \right] E_{\theta 1}^i + \sum_n \left[ \begin{matrix} a_n \\ -\beta_n a_n \end{matrix} \right] E_{\theta n}^i + \int_0^\infty \left[ \begin{matrix} q^r(\rho) \\ -\beta(\rho)q^r(\rho) \end{matrix} \right] E_\theta^i(\rho) d\rho \\ &= \int_0^\infty \left[ \begin{matrix} q^{t+}(\rho) \cdot (1-X) \\ \beta_1(\rho) \cdot q^{t+}(\rho) \cdot (1+X) \end{matrix} \right] E_\theta^t(\rho) d\rho \end{aligned}$$

where  $X = \Delta \cdot e^{-2j\beta_1(\rho)L}$

We use now the orthogonality properties between the modes of the same region in order to derive a set of coupled integral equations the unknown coefficients of which are  $a_n$  ( $n > 1$ ) and the unknown functions  $q^r(\rho)$  and  $q^{t+}(\rho)$ . After some algebraic manipulations we obtain:

$$\begin{aligned} q^{t+}(\rho) &= \frac{\pi |\beta_1(\rho)|}{\omega \mu_0 P} \frac{1}{(\beta_1(1-X) + \beta_1(\rho)(1+X))} \left[ 2\beta_1 \int_0^\infty r E_\theta^i E_\theta^{t*} d\rho \right. \\ &+ \sum_n a_n (\beta_1 - \beta_n) \int_0^\infty r E_{\theta n}^i E_\theta^{t*} d\rho \\ &\quad \left. + \int_0^\infty q^r(\rho') (\beta_1 - \beta(\rho')) \int_0^\infty r E_\theta^i(\rho') E_\theta^{t*}(\rho) d\rho' d\rho' \right] \\ q^r(\rho) &= \frac{\pi |\beta(\rho)|}{\omega \mu_0 P \beta(\rho)} \int_0^\infty q^{t+}(\rho') (\beta(\rho)(1-X) - \beta_1(\rho)(1+X)) * \\ &\quad \left. \int_0^\infty r E_\theta^t(\rho') E_\theta^{r*} d\rho' d\rho' \right] \\ a_n &= \frac{\pi}{2\omega \mu_0 P} \int_0^\infty q^{t+}(\rho) (\beta_n(1-X) - \beta_1(\rho)(1+X)) \int_0^\infty r E_\theta^t(\rho) E_{\theta n}^{t*} d\rho d\rho \end{aligned}$$

This system can be solved numerically by means of an iterative procedure based upon successive approximations on the scattering mechanism which has been detailed elsewhere [5].

#### NUMERICAL RESULTS ON DISCONTINUITIES

Fig 2 shows the loci of the reflection coefficients in the complex plane versus the normalized frequency  $fD$ . for the two types of discontinuities which can now be separately discussed. First, let us consider the substrate plugged rod case; Fig 2 illustrates the large variation of the phase of the reflection coefficient  $a_1$  versus the frequency and the weakness of the radiation loss ( $a_1 \sim 1$ ), whatever the value of the frequency.

The situation is quite different for the abruptly ended rod case. Since there is not metallic plane at  $z = L$ , the energy transferred to the radiating TE modes in region II can go to the infinity and we have more radiation losses than in the first case. For low normalized frequency values, the coupling between the guided TE<sub>01</sub> mode and the TE continuous modes as well as the radiation loss at the discontinuity are very high. As suspected, by increasing the normalized frequency, the reflection coefficient  $a_1$  in the latter case reaches the limit:

$$a_1 = \frac{\sqrt{\epsilon_r} + 1}{\sqrt{\epsilon_r} - 1}$$

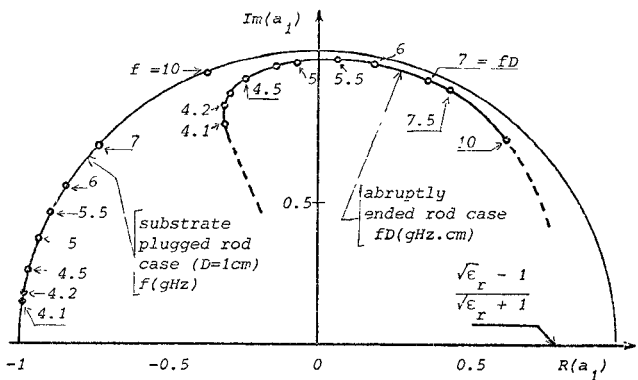


figure 2

#### THE DIELECTRIC RESONATOR PROBLEM

The electromagnetic parameters of the resonant magnetic dipole mode in a cylindrical dielectric resonator can be carried out from the rigorous analysis of the two interacting discontinuities we have studied separately just before. To do so, we could suppose for example that the excitation is a flow of continuous TE modes incident on the upper side of the resonator, so as to enlarge straightforwardly the previous rigorous formulation when studying this more complex case.

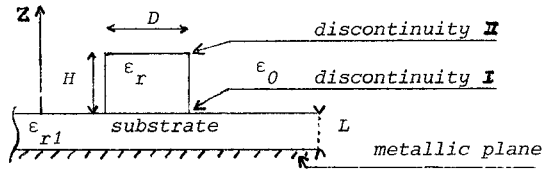


figure 3

It then becomes necessary to distinguish the discontinuity parameters  $a_n$  ( $n > 1$ ),  $q^r(\rho)$  and  $q^{t+}(\rho)$  by additive superscripts I and II, depending on their type at  $z = 0$  and at  $z = H$  (see fig.3)

The resonant frequency  $f_0$  of the magnetic dipole mode confined in the resonator can be derived from the stationary condition. The radiation  $Q$  factor can be determined either by the sharpness of the resonance curve versus the frequency, or by the basic definition:

$$Q = \frac{\text{reactive energy}}{\text{average radiated power}}$$

The theoretical study shows that the flow of continuous TE modes created by the discontinuity (I or II) which is incident on the second discontinuity (II or I) hardly couple any power on the TE<sub>01</sub> resonant mode.

According to this assumption, we can use directly the previous results obtained separately with the two types of discontinuities in order to determine the resonant frequency together with the radiation  $Q$  factor.

The  $Q$  factor can be expressed as

$$Q = 2\pi f H / [ v_g (1 - |a_1^I|^2) ]$$

for the isolated resonator ( $a_1^I = a_1^{II}$ ) and as

$$Q = 4\pi f \cdot H / [v_g (2 - |a_1^I|^2 - |a_1^H|^2)]$$

for the resonator on substrate. In above formulaes,  $v_g$  denotes the group velocity of the guided  $TE_{01}$  mode in the dielectric rod.

#### RESULTS ON CYLINDRICAL DIELECTRIC RESONATORS

Figure 4 illustrates the variations of the radiation  $Q$  factor and of the resonant frequencies isolated resonators ( $\epsilon_r = 35$  and  $\epsilon_r = 65$ ) versus the parameter  $D/H$  for which some theoretical data are available from [3]. Our values of the radiation  $Q$  factor are found about twice greater than VAN BLADEL's predictions. The optimum of the  $Q$  factor is obtained for  $D/H$  comprised between 1.3 and 1.5.

Figure 5 shows the behavior of the resonant frequencies of the  $TE_{01}$  mode for the isolated and on substrate resonators and for two values of the permittivity ( $\epsilon_r = 35$  and  $\epsilon_r = 65$ ). Our experimental results are in good agreement with the theoretical predictions.

On the figure 6, we present the variations of the radiation  $Q$  factor and of the diameter  $D$  for the resonator placed on an alumina substrate ( $\epsilon_{r1} = 9.6$ ;  $L = 0.635$ ) versus the quantity  $D/H$  for a given resonant frequency  $f = 5\text{GHz}$ . In this case, the optimum of the  $Q$  factor is obtained for  $D/H$  comprised between 1 and 1.3

#### REFERENCES

- [1] ITOH and RUDOKAS "New method for computing the resonant frequencies of dielectric resonators" European Microwave Conference ROME 1976
- [2] GUILLOU and CARAULT "Accurate resonant frequencies of dielectric resonators" IEEE Trans. Microwave Theory Tech., vol MTT-25, n° 11, November 1977
- [3] VERPLANKEN and VAN BLADEL "The magnetic dipole resonance of ring resonators of very high permittivity" IEEE Trans. Microwave Theory and Tech., vol MTT-27, n° 4, April 1979
- [4] MARCUSE "Radiation losses of the dominant mode in round dielectric waveguide" BSTJ vol 49 n° 8, p 1665 October 1970
- [5] GELIN, PETENZI and CITERNE "New rigorous analysis of the step discontinuity in a slab dielectric waveguide" Electron. Letters, vol 15, n° 12, pp 355-356 June 79

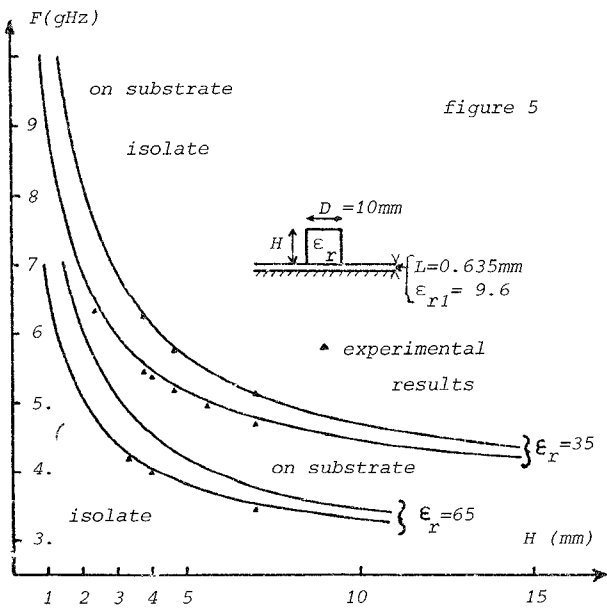


figure 5

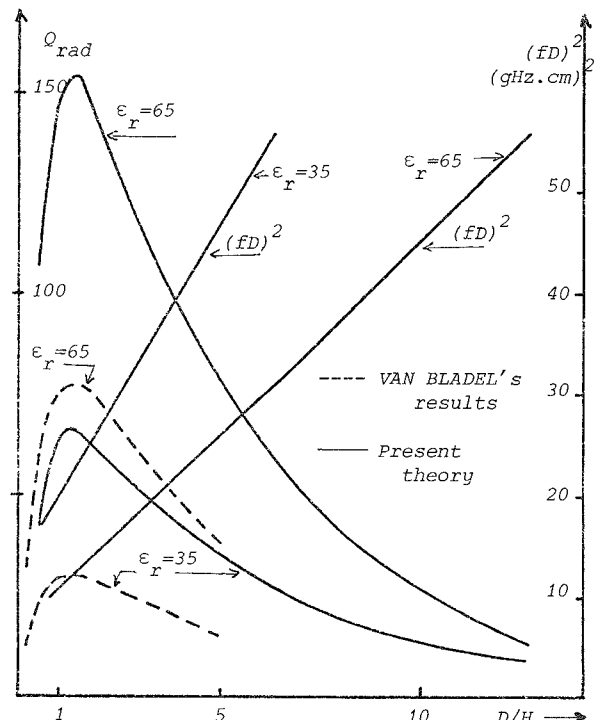


figure 4

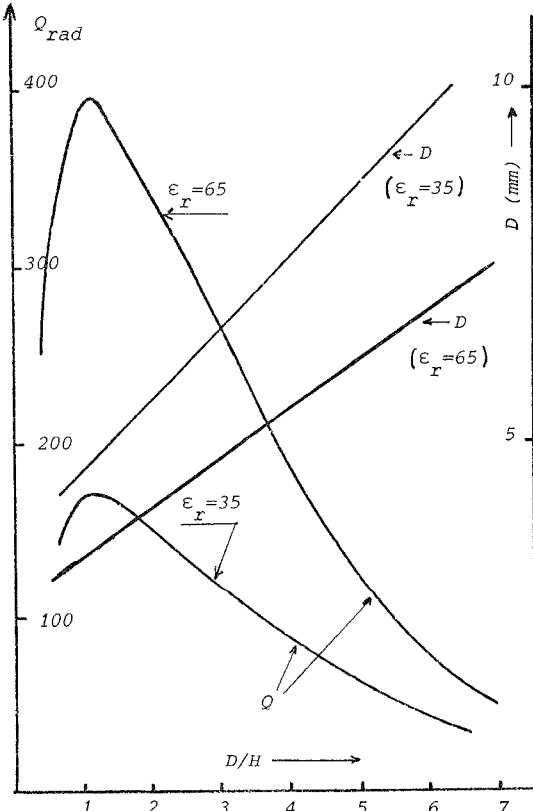


figure 6